Low Cost condition assessment method for existing RC bridges

Flavio Stochino*, Maria Luisa Fadda, Fausto Mistretta

Department of Civil, Environmental Engineering and Architecture, University of Cagliari. ITALY.
*Corresponding author, fstochino@unica.it

Abstract

Aging infrastructures represent a current engineering challenge. Huge budgets are necessary to keep their functionality and the lack of a proper and timely maintenance entails an increasing deterioration and therefore higher repair costs. Therefore, assessing the reliability of infrastructures becomes mandatory, with particular attention to the ones still in service even when their life limit has exceeded.
This paper aims to propose a new, fast and low cost method of condition rating for reinforced concrete bridges. This is based on visual inspection and non-destructive testing.
The main innovation is represented by the parameters taking into account the mechanical degradation of materials and the damage location at the structural sub-component level.
The analysis of some benchmark examples and the comparison with other methods are presented in order to assess the reliability of the new proposal.

Keywords
Degradation, Failure diagnostics, Residual life, Maintenance, Non-destructive inspection.

1 Introduction

Aging infrastructures has become a paramount problem nowadays, particularly in countries, like Italy, where the main motorways were built more than 50 years ago. The infrastructure functionality closely depends on a good inspection activity. In addition, lacks of a proper and timely maintenance entail an increasing deterioration and, consequently, higher repair costs.
Therefore, assessing the reliability of infrastructures becomes mandatory, with particular attention to the ones still in service even when their life limit has exceeded.
Investments for the development of a reliable Bridge Management System (BMS) have recently increased. BMS is the set of inspection, investigation, maintenance and repair of a group of bridges or viaducts, organized according to priority, with the support of computer databases and algorithms. Usually, the conservation of a structure is assessed through qualitative judgments. As a matter of fact, bridge rating or scoring is a tool used in BMS to prioritize maintenance investments. The BMS estimates the bridge relevance at a project or network level, considering its serviceability and importance in the road network in order to prioritize maintenance activities, see [1].
An early approach to this problem was presented [2] by Znidaric and Perus, who analysed the condition rating techniques for Reinforced Concrete (RC) bridges. They suggested that a condition rating method should not be based on the simple scoring of the inspected members (or of the whole structure), but on the numerical evaluation of all those essential damage types revealed during the inspection, whose character, intensity and extent may have a substantial impact on the safety and durability of the inspected structural member or structural component.
Gattulli and Chiaramonte, see [3], enriched the approach introduced in [2] including the evaluation of steel and masonry bridges and assessing the condition of each subcomponent in an overall structural system. Also Kano and Morikawa, see [4], applied the above-mentioned condition rating system to some cases of RC structures damaged by chloride induced deterioration. In particular, they introduced an interesting parameter representing the uncertainties of the inspection results.
In [5] the spatial time-dependant reliability analysis was merged with visual inspection in order to predict the likelihood of RC corrosion-induced cracking.

Please cite this paper as: Stochino, F., Fadda, M.L., Mistretta, F. Low cost condition assessment method for existing RC bridges (2018) Engineering Failure Analysis, 86, pp. 56-71.

One of the declinations of the approach presented in [2] is the Slovenian Method. More details will be given in Section 2.3. In [6] Kušar and Šelih considered a huge set of bridges to point out that climate and exposure to water are the most important parameters influencing the bridge condition.
Quite different methods have been proposed to prioritize bridges and suggest maintenance strategies at a network level. In [7] an index is presented, called Integrated Bridge Index IBI that takes into account the vulnerability risk and the strategic importance of each net component. The index was calibrated through visual inspections, experts' surveys, and regression analysis.
A method for a fast and automatic evaluation of the bridges stability and resilience is presented in [8], while a ranking strategy based on a multi-attribute utility theory (MUAT) is proposed in [9]. Some interesting results have been obtained using fuzzy logic, see [10] and [11].
Particular attention should be drawn on bridges with historical value; in this case the priority queue should consider the cultural importance of these structures as well. Two very interesting papers dealing with this topic are [12] and [13].
The idea of using several sources of information for the data necessary to rank the infrastructure conditions has been thoroughly investigated in literature. For example, detailed information on the geometry and displacements of the bridge by means of laser scanners, see [14-15], can be useful and relevant.
The Non-Destructive Techniques (NDT) can produce another important set of information contributing to complete the visual inspection data and reducing the dependency on the inspector's judgement. A very interesting paper dealing with this topic is [16], where a classification of the damage levels, assessment flowcharts and NDT methods results are presented. Significant examples of these techniques applied to historical bridges are also present in the literature: [17-20]
In this paper, the authors present an improved version of the early method described in [2] which takes into account the mechanical degradation of materials and the damage location. This would allow a fast and low-cost condition rating of the RC bridge network that can be easily implemented in BMS.
The present paper is organized as follows: in Section 2 the proposed method is presented along with two other methods based on [2], necessary for a comparison. Section 3 further analyses four benchmark real case studies to show the efficacy of the proposed approach. Finally, perspectives and conclusive remarks are drawn in Section 4.

2 Methods
2.1 Proposed Method

The assessment method proposed in this paper is divided into three main steps. In the first one a thorough visual examination is performed in order to detect any damages on the structure. Then, a set of non-destructive tests is developed in order to determine the mechanical characteristics of materials. Finally, the results of the first two steps are merged and analysed in order to obtain a Condition Rating Number *CRN* characteristic of each structure. It is a non-dimensional number related to the damage degree in the analysed structure. It is defined as follows:

$$CRN = \gamma\left(\frac{\sum_{m=1}^{k} F_{D\,m}}{\sum_{m=1}^{k} F_{D,ref\;m}}\right)\cdot 100 \tag{1}$$

where γ is an arbitrary scale constant that needs to be tuned for the considered case; F_{Dm} is the condition rating number for the m-th structural component while $F_{D,ref\;m}$ is the corresponding maximum value.
The definition of F_{Dm} is expressed by the following equation:

$$F_{Dm} = K_m \sum_{i=1}^{n} B_i \cdot K_{2i} \cdot K_{3i} \cdot L_i \cdot T_i. \tag{2}$$

K_m is a coefficient representing the importance of the considered element in the structure. Its values are reported in the Appendix: Table A1, extracted from [2]. B_i denotes the potential effect on the structural element safety of the i_{th} damage, see Table A2 in the Appendix. K_{2i} expresses the magnitude of the i_{th} damage divided into IV classes, from the lowest to the highest, whose values are reported in Table A3 (Appendix). K_{3i} represents the extension of the damage along the structural element, whose values belong to the range 0–1 according to the indications reported in Table A4 (Appendix).
An innovative aspect of this work is represented by the specification of the damage location and of the material properties degradation in each structural element. L_i and T_i can respectively measure these two aspects
L_i expresses the location of the i_{th} damage in the structural element and it can assume binary values: 1 in case it is not a critical point, 2 when it is a critical point, see Table 1. With "critical point", the authors mean the part of the single structural element that is "critical" for the structural safety. For example, the zones with the maximum stress values or with stress concentrations (beam midspan, support zones, holes etc.). Obviously, the critical points cannot be determined without knowing the boundary and loading conditions. Thus, for each different case a thorough assessment of this parameter is necessary.

Criterion	L_i
The damage is not located in a critical point	1
The damage is located in a critical point	2

Table 1. $\boldsymbol{L_i}$ parameter values representing the importance of the damage location.

T_i is the coefficient representing the material degradation. Its values are presented in the following Table 2 and they depend on the ratio between the design material strength f_{mk}^{d} and the one measured by experimental tests (e.g. rebound index, coring strength test, ultrasound pulse test etc.) f_{mk}^{exp}. When the former characteristic is not available, it is assumed equal to the minimum value required for the considered exposure class (see [21]). In case no experimental test can be developed on the structural element, the value of T_i is 4, for safety's sake. Considering RC structures, f_{mk} represents the concrete compressive cylindrical strength as a first approximation. Only in case further information on the reinforcements are available, it is the weighted average of the concrete and steel mechanical properties as expressed in equation (3):

$$f_{mk} = f_{ck} + f_{yk} \cdot \frac{E_c}{E_s}, \tag{3}$$

where f_{ck} and E_c are respectively the concrete characteristic strength and Young's modulus, while f_{yk} and E_s are the ones corresponding to steel. Equation (3) gives f_{mk}^{d} when the materials design values are used, while it yields to f_{mk}^{exp}, when the experimental mechanical characteristics are considered.

Criterion	f_{mk}^{exp}/ f_{mk}^{d}	T_i
High resistance	>1	1
Poor resistance	from 0.66 to 1	2
Low resistance	from 0.33 to 0.66	3
No resistance	from 0 to 0.33	4

Table 2. T_i values representing the material characteristics degradation.

In order to determine the extreme values of L_i and T_i a sensitivity analysis has been developed. Its

main results show that the lower is the maximum value of the parameter, the bigger is its influence on the CRN of the structure, see equation (1). Indeed, the denominator of the latter expression will report the parameters maximum values representing the damages. Thus, higher maximum values will produce lower *CRN* and vice versa. Given that the damage location can be determined with a rather high accuracy only by the visual inspection, while the material degradation cannot be easily assessed in many cases, in the authors' view L_i should have more importance than T_i. Consequently, the maximum value of L_i is lower than the maximum value of T_i.
For clarity's sake, the proposed method can be summarized as follows, see Fig. 1. In the first step, the considered structure should be divided in sub-components (column, beam, piers etc). Each sub-component has a different weight for the whole structure safety, represented by K_m.
For each component, information has to be further collected by analysing the design documentation and performing visual inspections or (where possible) experimental testing.
Any damage in each structural component should be rated considering its importance (B_i), magnitude (K_{2i}) and extension (K_{3i}) along with its position (L_i) and the corresponding material degradation (T_i).
Visual inspection can be developed using a damage identification form, like the ones reported in the Appendix: Tables A5, A6, A7, respectively for Abutment, Beam and Slab. Considering the framework of infrastructure monitoring, the first assessment of the structure should be performed by an experienced engineer, since the choice of B_i corresponding to damages is of paramount relevance. Indeed, for some sub-components (e.g. beams), some damages are less important than others, while for other sub-components (e.g. piles) the order of importance can be inverted.
According to the obtained *CNR* value the structure can be classified into one of the 4 damage categories, where a higher value corresponds to a worst condition, see Table 3.

Damage categories	***CRN/γ***
In service	0.00 -1.36
Little deterioration	1.36 -1.86
Severe deterioration	1.86 – 2.27
Urgent intervention	2-27 – 2.95
Out of service	>2.95

Table 3. Damage categories for the proposed method.

In order to check the reliability of the proposed approach, two classical methods adopted in Europe will be described: the Austrian method and the Slovenian one, see [2]. These two approaches were selected for comparisons because they have a similar conceptual framework (importance of damages, magnitude, extension, urgency) with respect to the new proposal.

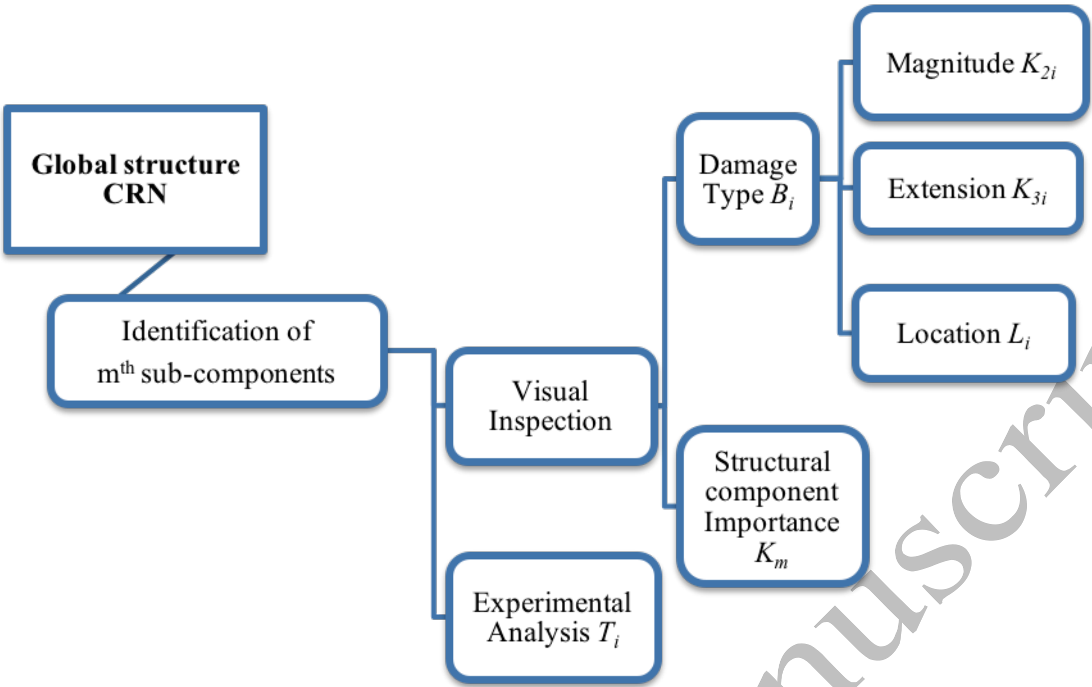

Figure 1. Condition Rating Number assessment scheme.

2.2 Austrian Method

This method was introduced by the Austrian Ministry for economic affairs, see [2] and [22]. These documents present the procedures and instructions for the condition assessment of bridge structures. The Austrian method proposes a numerical indicator representing the state of the bridge: the Condition Rating (CR_A). It is a numerical value (varying between 0, best condition, and 70, worst condition) that divides every kind of damage detected during the visual inspection into 32 groups and considers their severity and extent. It can be expressed by the following equation (see [2]):

$$CR_A = \sum_{i=1}^{32} G_i \cdot K_{1i}^A \cdot K_{2i}^A \cdot K_{3i}^A \cdot K_{4i}^A, \quad (4)$$

where: G_i represents the type of damage in the range of 1-5. K_{1i}^A denotes the damage extent. It is expressed by numerical values between 0 and 1. K_{2i}^A expresses the damage intensity with numerical values between 0 and 1. K_{3i}^A represents the importance of the structural sub-component or member, its values ranging between 0 and 1. K_{4i}^A denotes the urgency of intervention with a value between 0 and 10, depending on the structure type and on its collapse risk. According to the value obtained, the structure is classified into one of the 6 damage categories, see Table 4.

Damage categories	***CR_A***
Very little deterioration	0 – 3
Little deterioration	2 – 8
Medium deterioration	6 – 13
Severe deterioration	10 – 25
Very severe deterioration	20 – 70
Total deterioration	>50

Table 4. Damage categories for the Austrian method.

Please cite this paper as: Stochino, F., Fadda, M.L., Mistretta, F. Low cost condition assessment method for existing RC bridges (2018) Engineering Failure Analysis, 86, pp. 56-71.

2.3 Slovenian Method

According to the Slovenian method, see [2] and [6], the condition rating function (R) of a bridge structure can be assessed through the following expression:

$$R = \sum V_d = \sum B_i^S \cdot K_{1i}^S \cdot K_{2i}^S \cdot K_{3i}^S \cdot K_{4i}^S \ , \tag{5}$$

where: V_d is the value of the damage type, B_i^S represents the effect of the i-th damage type on the safety of the structural component, its value ranging from 1 to 4. K_{1i}^S takes into account the effect of the structural component on the whole structure, with values ranging from 0.1 to 0.4. K_{2i}^S denotes the intensity of the i-th damage type in a scale from 0.5 to 2. K_{3i}^S denotes the extension of i-th damage on the structural member, its values ranging from 0.5 to 2. Finally, K_{4i}^S represents the urgency of the intervention in case the i-th damage jeopardises the structure safety, with values between 1 and 5.
In this case, the condition rating (CR_S) can be expressed as a ratio between the effective sum of the damage values (ΣV_d) calculated for the observed structure and the reference sum of the damage values ($\Sigma V_{d,ref}$) obtained by taking into account every damage type potentially occurring on the same structure, multiplied by unit values of the extent and urgency factors:

$$CR_S = \frac{\Sigma V d}{\Sigma V_{d\,ref}}\ 100, \tag{6}$$

The value of CR_s allows classifying the analysed structures in one of the categories presented in Table 5:

Damage class	Definition	CR_s value
1	Normal condition	0-15
2	Retrofitting needed	15-25
3	Urgent intervention	25-50
4	Out of service	>50

Table 5. Damage classes and Condition Rating value for the Slovenian method.

3 Case Studies

In order to test the new proposed method, four real case studies have been analysed. These were selected because, in most cases, the data sets were quite complete and all the required coefficients could be estimated. In each case, the condition rating estimation was developed using the proposed method, see Section 2.1, and the known Austrian and Slovenian methods, see Section 2.2 and Section 2.3. For simplicity's sake, the value of γ=22, see equation (1), was chosen for the analysed case studies. This is a totally arbitrary value; nevertheless, it can contribute to more understandable results for political decision-makers. Actually, it should be tuned for each infrastructure net considered.

3.1 P20C Bridge in Segariu (Italy)

The P20C bridge spans over the main supply canal bringing water from the Flumendosa Systems to the plain of Campidano in Sardinia (Italy). It has a single span 10 m long and is composed of a deck supported by 1 transversal and 5 longitudinal beams simply supported by two abutments. The material used is reinforced concrete casted on site, considering the exposition class X4, see [21], the

minimum design compressive strength has been rated equal to 40 MPa. The FeB44k reinforcement steel is characterized by a yielding stress equal to 440 MPa. The main geometrical characteristics and reinforcements distribution can be seen in Figure 2. In particular, the deck presents a transversal cantilever 70 cm long that is heavily exposed to rain.
The general condition of the bridge is quite good, as Figure 3 shows. The deck is the part presenting rather large humidity spots and diffused concrete spalling, leading to the environmental exposition of some stirrups.

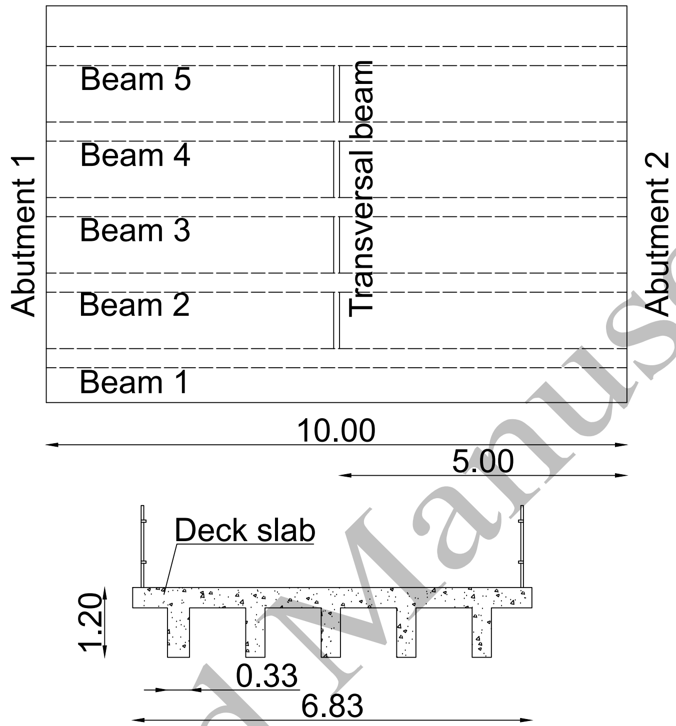

Figure 2. Geometry of the P20C bridge, plant view (top) and transversal cross section (bottom).

(a) (b) (c)
Figure 3. Views of the PC20 bridge conditions, (a) abutment 1, (b) midspan, (c) abutment 2.

A synthesis of the condition of each structural component has been reported in Table 6. This also shows the reference and actual damage rating for each element. The ratio between these two values, reported in the last column, can highlight which components are in the worst condition. As expected, the little damages assessed do not strongly influence the safety of any structural component.

Structural Component	K_m	$F_{d,ref\,m}$	F_{dm}	$F_{dm}/F_{d,ref\,m}$
Abutment 1	0.4	512.0	9.6	0.02
Abutment 2	0.4	512.0	2.4	0.01
Deck slab	0.4	320.0	13.4	0.04
Transversal beam	0.3	240.0	4.8	0.02
Beam 1	0.6	499.2	4.2	0.01
Beam 2	0.6	499.2	6.0	0.01
Beam 3	0.6	499.2	11.1	0.02
Beam 4	0.6	499.2	11.1	0.02
Beam 5	0.6	499.2	12.9	0.03

Table 6. Rating of the various components of the P20C bridge.

Interestingly, in this case some experimental tests could be developed to assess the concrete mechanical characteristics, see Table 7. Thus, the values of T_i have been directly calculated: they are equal to 2 in every case. In addition, damages were not located in critical positions and consequently L_i is equal to 1. For beams presenting different concrete compressive strengths related to different zones of the elements, the lower values have been selected to produce a conservative condition rating number estimation.

Deck zone	Sclerometer (MPa)	Pull out (MPa)	Ultrasound pulse velocity (m/s)	Ultrasound on cores (m/s)	Compression strength test on cores (MPa)
Near abut. 1	39.72	36.32	1697	3610.1	31.85
Midspan	43.54	40.01	1413	3413	42.04
Near abut. 2	42.35	41.29	1588	3413	36.94

Table 7- Concrete materials tests developed on the P20C bridge. For clearness ‘sake: the sclerometer measures are based on the SonReb method [23-24], the ultrasound pulse velocity is directly measured on the structure in situ, while the ultrasound pulse velocity on cores is measured on the cores extracted from the structure.

Finally, the *CRN*, CR_A and CR_S have been calculated using the above-mentioned methods, see Table 8. In every case, the condition rating yields to a serviceable condition class. For this reason, ordinary maintenance is expected in order to further reduce the damage extension.

Structure	Proposed Method	Austrian Method	Slovenian Method
Whole structure	40.7	3.8	18.5
Condition	Little deterioration	Little deterioration	Retrofitting needed

Table 8- Condition ratings of the whole P20C bridge obtained with the three analysed methods.

3.2 Concorde bridge in Laval Quebec

The Concorde bridge in Laval (Montreal, Quebec) is an overpass over the Canadian Highway 19. It is composed of 20 pre-stressed concrete box girders, 28 m long, supporting a 24 m width deck slab, see Figure 4. It was casted on site and covered with a waterproofing membrane and asphalt pavement. Two abutments located at its ends support the overpass. An inclined frontal wall and four longitudinal retaining ones compose each abutment. The latter support a thick cantilever slab, which is connected to the deck slab with an expansion joint. On September 30th 2006 the Concorde bridge collapsed causing five victims and six injured, see [25].

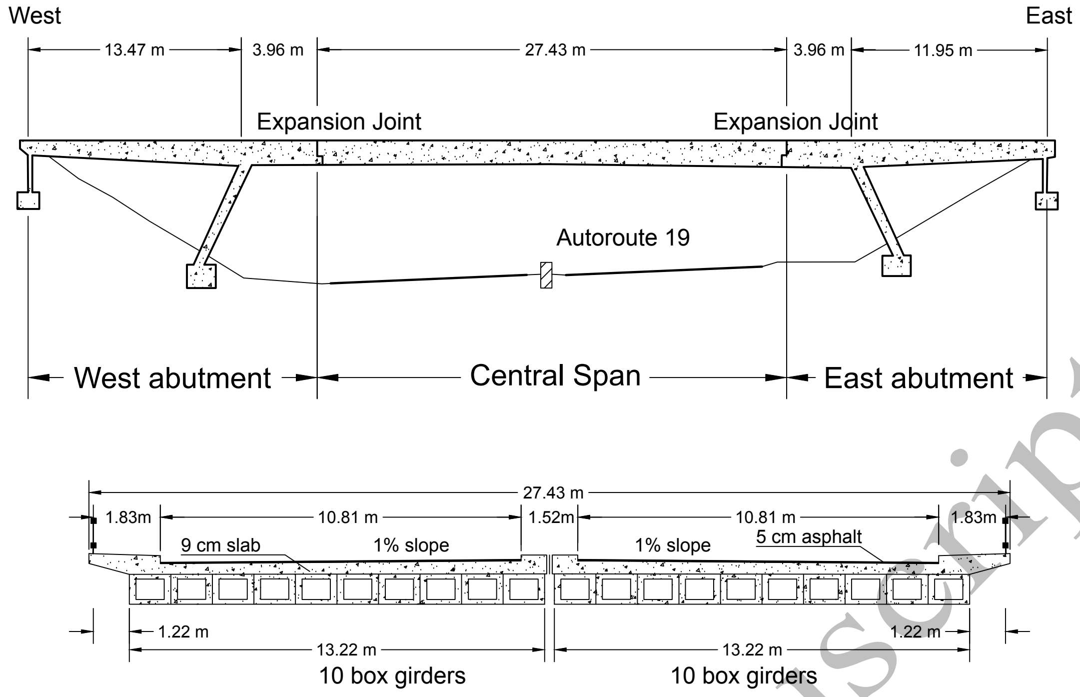

Figure 4. Longitudinal (top) and cross sections (bottom) of the Concorde Bridge. .

The overpass was built in 1970 and many inspections performed during its service life are reported in [25]. The first recorded inspections (1977-1978) did not show any relevant abnormality. In 1980 a leaking expansion joint was identified but reports from 1982 and 1984 present the overpass in good conditions. Inspections from 1985 to 1991 presented the Concorde Bridge with small signs of deterioration, but the general judgment on its safety was good. In 1992 the overpass showed significant damages, both expansion joints were defective and patched, the pavement was cracked in many points. On the east abutment, see Figure 4, the concrete scaling had occurred while on the northeast lateral face reinforcements were exposed after concrete spalling. In addition, on the lateral face of the southeast abutment a shear crack was clearly detected. The beam seats degradation was underlined but this part of the bridge could not be closely inspected.
In addition, in 1992 some repairs were made, but the report [25] describes them as of a “dubious quality” (e.g. the shotcrete used obstructed the expansion joint). In 1997 there was the first clear reference to cracks on the cantilever slab. The main warnings aroused from the 2004 report, where a major beam seat degradation and wide shear cracks on the cantilever were assessed. The ultimate inspections were developed in 2005, confirming the main warnings and assessing a “mediocre” general condition of the overpass. The collapse happened on September 30th 2006, as a result of a shear failure of the south-east cantilever under its own weight. The deterioration of the concrete was the main cause behind this tragic event. The freeze-thaw cycles in addition to the de-icing salts produced may have caused the material degradation in this area and consequently a crack inside the thick cantilever slab.
The proposed method was applied to this case study; pictures and details reported in [25] and [26] have been analysed. In particular, the design concrete compressive strength for the cast on site slab was 27.8 MPa, while the design yield stress for reinforcements was 276 MPa. Unfortunately, there were not any data from materials strength assessments, but, as reported in [25]: the inquiry commission agrees with the experts’ consensus and believes that the confusion created by not clear material specifications “resulted in the use of low quality concrete, which progressively deteriorated under the influence of freeze-thaw cycles in the presence of de-icing salts.” Thus, to take into account this information the value of T_i has been considered equal to 4 for each structural component. In addition, the location parameter L_i was carefully evaluated for each case. For example, considering the importance of the beam seats L_i =2 was assumed for all the damages in

this zone, while a unit value was assumed for the damages in other parts of the abutments.
The damage identification forms, reported in Tables A5-A7 (Appendix), were compiled considering 4 main substructures: the two abutments, a generic girder beam, representative for all 20 ones and the deck slab. This compensated for the lack of information on the specific conditions of each beam. Table 9 reports a synthesis of the results concerning each structural component. As shown, the east Abutment collects the highest value of $F_{dm,}$ which is the condition number characteristic of each sub-component as defined in equation (2). This part clearly represented the main problem for the overpass, while damages in the other parts seem not to be too heavy. Developing this kind of analysis can contribute to optimize the maintenance costs, allowing a shorter infrastructure service interruption and an analysis focused on the most deteriorated parts of the bridge.

Structural Component	K_m	$F_{dm\ ref}$	1984	1991	1992	1997	2004	2005
Abutment East	0.4	512	0.0	1.6	24.0	67.2	89.6	89.6
Abutment West	0.4	512	0.0	0.0	14.4	14.4	19.2	19.2
Girder beam	0.6	499	0.0	0.0	4.8	4.8	9.6	19.2
Deck slab	0.4	320	0.0	0.0	0.0	7.2	9.6	9.6

Table 9. F_{dm} values for the structural components of Concorde bridge according to the different reports, the first two columns represent the K_m parameter and the reference value $F_{d,mref}$.

The global *CRN* (defined in equation (1)) was compared to the rating obtained with the other two methods presented in Section 2: Austrian, (equation 4) and Slovenian, (equation 6) methods. Figure 5 presents this comparison for each condition rating estimation based on the above-mentioned inspection reports. Every method underlines a dangerous situation after 1997, suggesting caution to the bridge conditions. The new proposed method allows emphasizing this degradation with high gradients of the *CRN*.

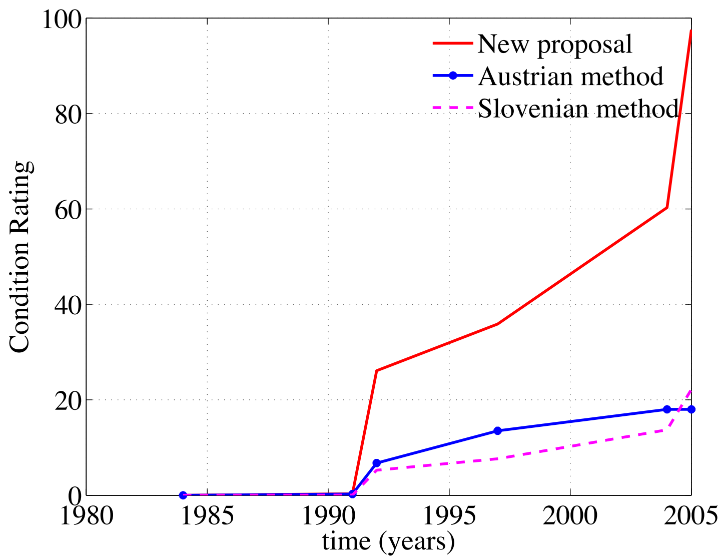

Figure 5. Condition ratings of the Concorde Bridge in Laval Quebec based on the methods presented in Sec. 2 (new proposal, Austrian method, Slovenian method).

3.2 Lake View Drive Bridge

On December 27th 2005 the east-side edge beam of the Lake View Drive Bridge in Washington Pennsylvania, collapsed falling on the highway below. Fortunately, no damages to people were reported. Heavy spalling and corrosion of the strands on the bottom flange of the failed midspan non-composite pre-stressed concrete box beam member were assessed by the post-collapse inspection. In addition, corrosion problems were revealed on other box beams and the bridge was

Please cite this paper as: Stochino, F., Fadda, M.L., Mistretta, F. Low cost condition assessment method for existing RC bridges (2018) Engineering Failure Analysis, 86, pp. 56-71.

subsequently removed from service.
The bridge was built in 1960 and its geometry is depicted in Figure 6: it is composed of 32 box beams distributed over 4 spans and supported by 3 piers and 2 abutments. Many interesting details can be found in [27-29]. The 1953 Standard Specification for Highway Bridges [30] was adopted to design the bridge. The box beams, characterized by a hollowed cross section 123x106 cm, see Figure 6, were pre-stressed by Grade 250, 3/8-in diameter, seven-wire strands. Naito et al [27] point out that the designed strand cover did not violate the prevailing design specification, but the section cuts extracted from 3 box beams reveal that the average clear cover is less than 60% of the designed amount. Furthermore, the stirrups were placed between the bottom and the secondary layers of strand; consequently they cannot contain spalling.

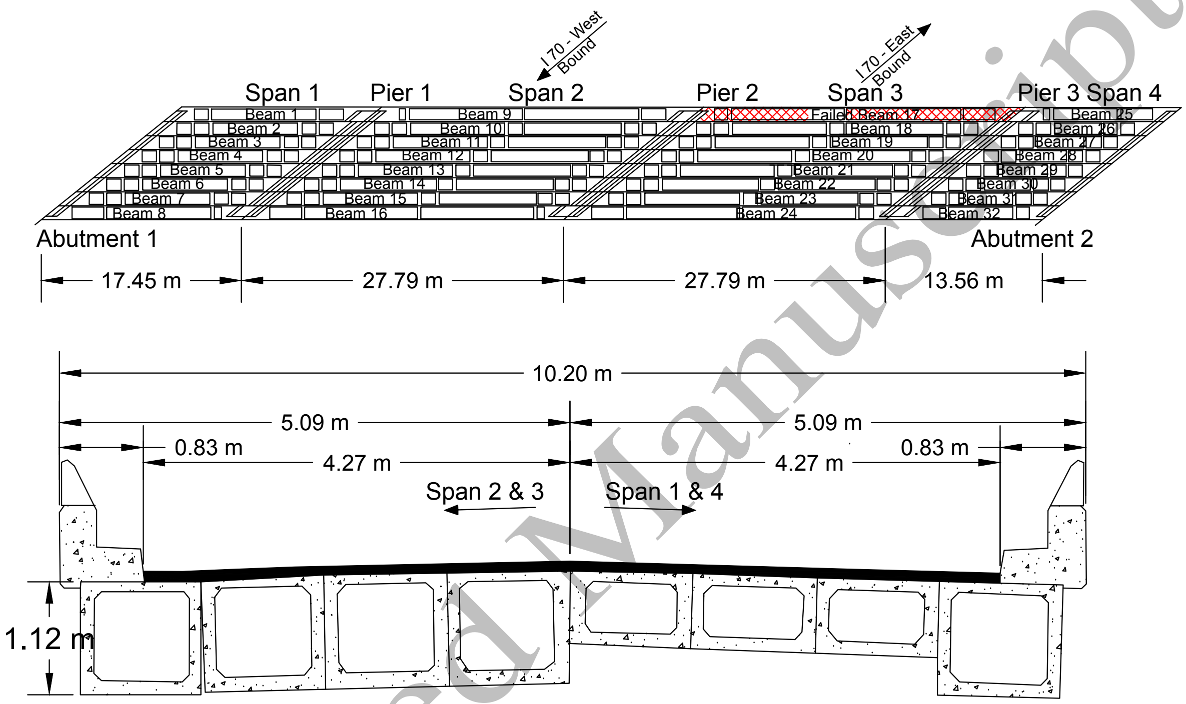

Figure 6. Geometry of the Lake View Drive Bridge, conceptual view (top) and cross sections (bottom). The collapsed beam 17 is highlighted in red.

The design concrete compressive strength was 40.7 MPa at 28 days and 33.8 MPa at the transfer of the pre-stress. After the collapse, concrete cores were taken from some beams. The compressive strength of these specimens varied between 42.7 to 57.9 MPa, confirming the good quality of the materials. For this reason, the material degradation parameter T_i has been rated equal to 1 for this case.
The post collapse report by Harlte [29] revealed that most of the pre-stressing tendons showed corrosion, probably induced by chloride attacks. Indeed, the water leakages from the bridge deck through shear keys, between adjacent box beams, were not well fabricated.
The rating condition number *CRN* was evaluated for this structure along with the CR_S and CR_A. The main results are reported in Table 10. The whole structure presents very high condition rating, corresponding to high degradation and indicating that it is out of service. Interestingly, the damages presented in [27] and [29] for the failed beam 17 (see Fig 6) produce a condition rating about twice the value of the other generic damaged beams. The three methods show quite a good agreement in this case.

Structure	Proposed Method	Austrian Method	Slovenian Method
Whole structure	116.4	519.7	105.8
Beam 17	57.6	31.5	288.0
Generic beam	28.8	15.8	144.0

Table 10- Condition ratings of the whole structure, the collapsed beam 17 and a generic beam obtained with the three analysed methods.

3.3 Charlotte Motor Speedway Pedestrian Bridge

The Charlotte Motor Speedway Pedestrian Bridge collapsed on May 20th 2000 under the load of a walking crowd, injuring 107 people. It was a four span, simply supported, precasted and prestressed reinforced concrete bridge spanning a major US highway, see Figure 7. Many interesting details can be found in [31] and [32]. The main cause of the collapse may have been a chloride attack causing the prestressing tendons corrosion on the double T beams. This was assessed on the failed span of the bridge, with the same problem expanding also to other spans. Indeed, [32] presents pictures showing a clearly visible longitudinal crack directly under the grout plug location and in many other parts of the bridge that had not collapsed.

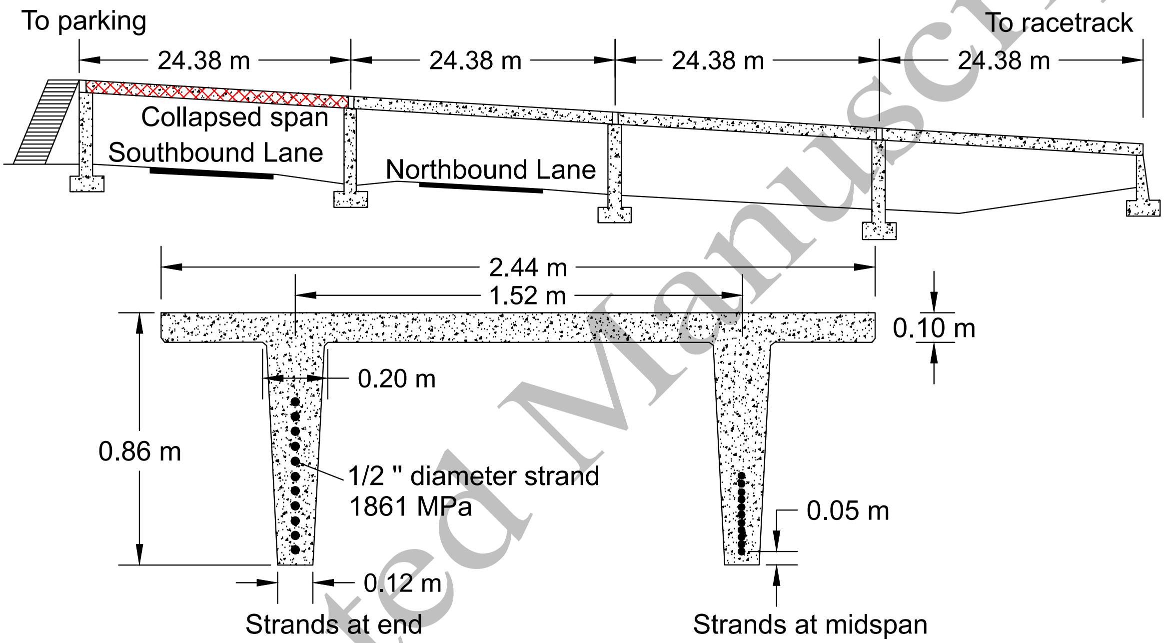

Figure 7. Geometry of the Charlotte Speedway Pedestrian Bridge. Longitudinal view (top), transversal cross-section (bottom), the collapsed span is highlighted in red.

Structure	Proposed Method	Austrian Method	Slovenian Method
Whole structure	109.19	24.0	24.82
Condition	Out of service	Severe Deterioration	Retrofitting needed

Table 11- Condition ratings of the whole Charlotte Motor Speedway Pedestrian Bridge obtained with the three analysed methods.

The three condition rating methods were applied to this case as well; their results are reported in Table 11. The *CRN*, CR_A and CR_S are very high, confirming the bad condition of the collapsed bridge.

Considering the new proposed method, the material degradation parameter T_i, and the location parameter L_i have been respectively rated equal to 4 and 2 for the beams. Indeed, no direct information was found about the concrete compressive strength and the position of the longitudinal cracks leads to assume the maximum values for the above-mentioned parameters. Looking at Table 11 the proposed method clearly highlights the gravity of the situation. Indeed, the introduction of T_i and L_i allows pointing out the weak points of the bridge with a greater flexibility.

5 Conclusions

This paper aims to propose a new fast and low cost condition rating method for RC bridge network. This is based on visual inspection and NDT testing and can be synthetized as follows.
After the identification of each structural element, information for the condition rating assessment needs to be collected, examining the design documentation and performing visual inspection and (where possible) experimental testing (NDT etc.). Indeed, any damage in each structural element should be rated considering its importance, extension and magnitude along with its position and the material degradation for this position. In addition, each structural element has a different weight for the whole structure safety. In this way, the analysed element can be ranked both at project level with reference to the same structure and at network level, considering more structures at the same time. Thus, the relative *CRN,* and not its absolute value, should be considered. Maintenance costs and service interruption can be optimized taking into account the priority queue built with this approach. Indeed, this method enables BMS decision makers to choose whether to retrofit the entire bridge or just its critical elements, reducing the *CRN* and optimizing the allocation of the available economic resources.
The main innovation is represented by the parameter taking into account the mechanical degradation of materials and the one accounting for the damage location at the structural elements level. Indeed, in the authors view, these two issues should be thoroughly considered in order to assess the structural safety.
The analysis of some benchmark examples and the comparison with other methods assessed the reliability of the new proposal.
Further developments are expected considering different kinds of materials, like steel and masonry [33-34], and episodic events like fire, see [24], and impact/blast load, see [35-39], that can reduce the service life and whose damages are not easily quantifiable.

6 References

[1] M.A. Zanini, F. Faleschini F., Pellegrino C. Cost analysis for maintenance and seismic retrofit of existing bridges, Structure and Infrastructure Engineering, 12(11) (2016) 1411-1427.
[2] J. Znidaric, I. Perus, Condition rating methods for concrete structures, CEB Bulletin No. 243: Strategies for Testing and Assessment of Concrete Structures, Appendix A (1998).
[3] V. Gattulli, L. Chiaramonte, Condition Assessment by Visual Inspection for a Bridge Management System, Computer-Aided Civil and Infrastructure Engineering 20 (2005) 95–107.
[4] H. Kano, H. Morikawa, Condition rating methodology on RC bridges with chloride induced deterioration. Reliability and Optimization of Structural Systems: Assessment, Design, and Life-Cycle Performance (2007) 113.
[5] Q. Suo, M. G. Stewart, Corrosion cracking prediction updating of deteriorating RC structures using inspection information, Reliability engineering & system safety 94(8) (2009)1340-1348.
[6] M. Kušar, J. Šelih, Analysis of bridge condition on state network in Slovenia, Građevinar 66 (9) (2014) 811-822.
[7] S. Valenzuela, H. Solminihac,T. Echaveguren, Proposal of an integrated index for prioritisation of bridge maintenance, Journal of Bridge Engineering 15 (3) (2010) 337-343.
[8] H.K. Liao; N.J. Yau, Development Of Various Bridge Condition Indices For Taiwan Bridge Management System, Proceedings of the 28th ISARC, Seoul, Korea (2011) 911-916.
[9] A. Dabous, S. Alkass, A multi-attribute ranking method for bridge management, Journal of Engineering, Construction and Architectural Management 17 (3) (2010) 282–291.
[10] F. Mistretta, V. Piras, M.L. Fadda, A reliable visual inspection method for the assessment of r.c. structures through fuzzy logic analysis, Life-Cycle of Structural Systems: Design, Assessment,

Maintenance and Management - Proceedings of the 4th International Symposium on Life-Cycle Civil Engineering (2014) 1154-1160.
[11] M.L. Fadda, F. Mistretta, V. Piras, Vulnerability Assessment of Concrete Bridges using Different Methods of Visual Inspection. Civil-Comp Proceedings (2014) 105, 1759-3433.
[12] B. Riveiro, P. Arias, J. Armesto, C. Ordóñez, A methodology for the inventory of historical infrastructures: documentation, current state, and influencing factors, International Journal of Architectural Heritage, 5(6) (2011), 629-646.
[13] M. Aflatooni, T. H. Chan, D. P. Thambiratnam, I. Thilakarathna, Synthetic rating system for railway bridge management, Journal of Civil Structural Health Monitoring 3(2) (2013) 81-91.
[14] P. Tang, B. Akinci, Formalization of workflows for extracting bridge surveying goals from laser-scanned data, Automation in Construction, 22 (2012) 306-319.
[15] G. Vacca, F. Mistretta, F. Stochino, A. Dessi, Terrestrial laser scanner for monitoring the deformations and the damages of buildings, International Archives of the Photogrammetry, Remote Sensing and Spatial Information Sciences - ISPRS Archives 41 (2016) 453-460.
[16] S.K.U. Rehman, Z. Ibrahim, S.A. Memon, M. Jameel, Nondestructive test methods for concrete bridges: A review, Construction and Building Materials 107 (2016) 58-86.
[17] O. Bergamo, G. Campione, S. Donadello, G. Russo, In-situ NDT testing procedure as an integral part of failure analysis of historical masonry arch bridges. Engineering Failure Analysis *57* (2015) 31-55.
[18] M. Solla, H. Lorenzo, B. Riveiro, F.I. Rial, Non-destructive methodologies in the assessment of the masonry arch bridge of Traba, Spain, Engineering Failure Analysis, 18(3) (2011) 828-835.
[19] O. Bergamo, G. Campione, C. Cucchiara, G. Russo,. Structural behavior of the old masonry bridge in the Gulf of Castellammare, Engineering Failure Analysis, 62 (2016) 188-198.
[20] O. Bergamo, G. Russo, S. Donadello, Retrofitting of the historic Castagnara bridge in Padua, Italy, with fibre reinforced plastic elements, Structural Engineering International, 24(4) (2014) 532-543.
[21] UNI EN 206-1:2006 Concrete - Part 1: Specification, performance, production and conformity.
[22] BRIME PL97-2220. Review of current practice for assessment of structural condition and classification of defects, Brussels (2001).
[23] D. Breysse, Nondestructive evaluation of concrete strength: An historical review and a new perspective by combining NDT methods, Construction and Building Materials 33 (2012) 139-163.
[24] F. Stochino, F. Mistretta, P. Meloni, G. Carcangiu, Integrated approach for post-fire reinforced concrete structures assessment, Periodica Polytechnica Civil Engineering 61(4) (2017) 677-699.
[25] P.M. Jhonson, A. Couture, R. Nicolet, Commission of inquiry into the collapse of a portion of the de la Concorde Overpass, Library and Archives Canada (2007)
[26] D. Mitchell, J. Marchand, P. Croteau, W.D. Cook, Concorde overpass collapse: structural aspects, Journal of Performance of Constructed Facilities, 25(6) (2011) 545-553.
[27] C. Naito, R. Sause, I. Hodgson, S. Pessiki, T. Macioce, Forensic examination of a noncomposite adjacent precast prestressed concrete box beam bridge, Journal of Bridge Engineering, 15(4) (2010). 408-418.
[28] C. Naito, J. Warncke, Inspection, Methods & Techniques to Determine Non Visible Corrosion of Prestressing Strands in Concrete Bridge Components: Task 1–Literature Review (2008)
[29] R. Hartle, Field Inspection and forensic investigation of the SR 1014 Lake View Drive Bridge over Interstate 70 final report, Michael Baker Jr. Rep., PennDOT, Harrisburg, Pa., 52 (2006)
[30] AASHTO (1953), Standard specifications for highway bridges, 6th Ed., Washington, D.C.
[31] R.W. Poston, J.S. West, Investigation of the Charlotte Motor Speedway bridge collapse. In Structures Congress 2005: Metropolis and Beyond (2005) 1-11.
[32] E. Proverbio, L.M. Bonaccorsi, Failure of prestressing steel induced by crevice corrosion in prestressed concrete structures. In, Proceedings of 9th international conference on durability of materials and components (9DBCM), Brisbane, (2002)

[33] P. Zampieri, M.A. Zanini, F. Faleschini, Derivation of analytical seismic fragility functions for common masonry bridge types: methodology and application to real cases, Engineering Failure Analysis, 68 (2016) 275-291.
[34] P. Zampieri, M.A. Zanini, F. Faleschini, L. Hofer, C. Pellegrino, Failure analysis of masonry arch bridges subject to local pier scour. Engineering Failure Analysis 79 (2017) 371-384.
[35] M. Acito, F. Stochino, S. Tattoni, Structural response and reliability analysis of RC beam subjected to explosive loading, Applied Mechanics and Materials*,* 82 (2011) 434-439.
[36] F. Stochino, RC beams under blast load: Reliability and sensitivity analysis. Engineering Failure Analysis 66 (2016) 544-565.
[37] W. Wang, D. Zhang, F. Lu, S. Wang, F. Tang, Experimental study and numerical simulation of the damage mode of a square reinforced concrete slab under close-in explosion, Engineering Failure Analysis 27 (2013) 41–51.
[38] R. Codina, D. Ambrosini, F. de Borbón, Alternatives to prevent the failure of RC members under close-in blast loadings, Engineering Failure Analysis 60 (2016) 96–106.
[39] D. Zhang, S.J. Yao, F. Lu, X.G. Chen, G. Lin, W. Wang, Y. Lin, Experimental study on scaling of RC beams under close-in blast loading, Engineering Failure Analysis 33 (2013) 497–504.

Acknowledgement
The authors acknowledge the financial support of the Autonomous Region of Sardinia under the L.R. 7/08/2007 Nr. 7 programme, the Italian Ministry of University and Research, the Conference of Rectors of Italian Universities and Confindustria, the Italian Industrial Federation, under the PhD-ITalents programme.

Appendix

Structural component	Structural member	K_m	$\sum$
Substructure, type I Pier	Piles (when inspectable)	0,2	
	Foundation or pile cap	0,3	
	Columns or wall	0,4	
	Pier cap	0,3	1,2
Substructure, type II Abutment	Piles (when inspectable)	0.2	
	Foundation or pile cap	0.3	
	Abutment wall	0,4	
	Backwall	0,1	
	Wingwalls	0,2	1,2
Superstructure, type 1 Girders	Girders	0,6	
	Deckslab	0,4	
	Enddiaphragms	0,2	
	Diaphragms	0,2	1,4
Superstructure, type 2 Stringers	Stringers	0,6	
	Deckslab	0,4	
	Enddiaphragms	0,2	1,2
Superstructure, type 3	Solid or voided slab	1,2	1,2
Superstructure, type 4 Box girder Arch	Top (deck) slab	0,4	
	Bottom slab	0,3	
	Webs	0,3	
	Diaphragms	0,2	
Bridge deck	Sidewalk	0,1	
	Barrier	0,2	
	Parapet		
	Median		
	Curb	0,1	0,4

Table A1: Factor K_m values for different kinds of structural members. Extracted from [2].

Item	Damage type	B_i	Degree of damage I	II	III	IV
1.0 Displacements and deformations of the structure						
1.1	**Substructure**					
1.11	Lateral movements	2	2 cm	from 2 to 5 cm	from 5 to 10 cm	>10 cm
1.12	Tilt, rotation, out of plumb	2	<1/100	from 1/100 to 3/100	from 1/100 to 5/100	>5/100
1.13	Differential settlement	3	<2 cm	from 2 to 5 cm	from 5 to 10 cm	>10 cm
1.14	Scoured area beneath pier/abutment	4	<10 %	from 10 to 25%	from 25 to 50%	>50%
1.2	**Superstructure**					
1.21	Vertical deflection	2	<L/1000	from L/1000 to L/500	from L/500 to L/300	>L/300
1.23	Unsmooth approach, bump	1		General criteria		
2.0 Concrete						
2.1	Poor workmanship: peeling, stratification, honeycomb, voids.	1	Single small defect	Several diff. small. defects simult.	Few stronger defects	Several different stronger defects
2.2	Plastic shrinkage and plastic settlement cracks, crazing, cracks caused by inefficient joints.	1	Single smaller	Several smaller	Few stronger	Many stronger
2.3	Strength lower than required	2	<10%	10 to 20%	20 to 30%	>30%
2.4	Depth of cover less than required for the ambient condition	2	<1 cm	1 to 2 cm	2 to 3 cm	>3 cm
2.5	Carbonation front (pH<10), with reference to the reinforcement level	2	2 to 3 cm above	1 to 2 cm above	0 to 1 cm above	At the level
2.6	Chloride penetration, with reference to the reinforcement level	3	>2 cm above	0.5 to 2 cm above	At the level	Below the level
2.7	Cracking caused by direct loading, imposed deformations and restraint	3	single <0,5 mm	several < 0,5 mm	single > 0,5 mm	several> 0,5 mm
2.8	Mech, Frommages; erosion, collision	1		General criteria		
2.9	Efflorescence, exudation, pop-outs	1		General criteria		
2.10	Leakage trough concrete	2	Light and medium	Heavy and sev. chlorid <0,4 % cem.	Light and medium	Heavy and severe chlorides > 0,4 %
2.11	Leakage at cracks, joints, embedded items	2	Ditto		Ditto	
2.12	Wet surface	1	Ditto		Ditto	
2.13	Freezing and thawing	2	weathering	cracking	spalling	disintegration
2.14	Freezing in presence of de-icing salts, scaling	2	Light < 1mm concrete skin	Medium 1 to 4 mm fine mortar	Heavy 4 to 10 mm aggr. exposed on surface	Sever >10 mm aggregate clearly exposed
2.15	Cover defects caused by reinforcement corrosion	2	Rust stains, light	Rust stains heavy	Crack cover stirrups	Delamination over stirrups
2.16	Spalling caused by corrosion of reinforcement (bars and prestressing tendons or ducts)	3	Finer cracks along reinforcement bars or tendons in corners	Finer cracks along other bars/tendons, cracks or exposed reinf. along corners	Wider cracks along other bars and tendons or exposed reinforcement	Bellow areas and surface spalling
2.17	Open joint between segments	2	<1mm	1 to 3 mm	3 to 5 mm	>5 mm
3.0 Reinforcing and prestressing steel						
3.1	Corrosion of stirrups	1		General criteria		
3.2	Corrosion of main reinforcing bars, reduction of steel area in the section	3	<10%	< 10%	electrolytic > 10%	pitting >10%
3.3	Duct deficiencies	2	Outside corrosion	Local voids, no chlorides	Larger voids no chlorides	Chlorides in the grout
3.4	Corrosion of prestressing tendons depth	4	≤ 1 mm	from 0,1 a 0,3 mm	from 0,3 a 0,5 mm	≥5 mm

Table A2: Factor B_i values for different kinds of damages. Extracted from [2].

Class	**Degree**	**Criterion**	K_{2i}
I	Low, initial	Damage is of small size, generally appearing on single localities of a member	0,5
II	Medium, propagating	Damage is of medium size, confined to single localities, or, damage is of small size appearing on few localities or on a small area of a member (e.g.<25%)	1
III	High, active	Damage is of large size, appearing on many localities or on greater area of a member (e.g. 25 to 75%)	1,5
IV	Very High, critical	Damage is of very large size, appearing on the major part of a member (e.g. >50%)	2

Table A3: Factor K_{2i} magnitude of the i[th] damage. Extracted from [2]

Criterion	K_{3i}
Damage is confined to a single unit of the same bridge member	0,5
Damage appears on several units (e.g. less than ¼) of the same bridge member	1
Damage appears on the major part of units (e.g. ¼ to ¾) of the same bridge member	1,5
Damage appears on the great majority of units (e.g. more than ¾) of the same bridge member	2

Table A4: Factor K_{3i} extension of the i[th] damage. Extracted from [2].

Damage	**B**	K_2	K_3	**L**	R_{ck}^{exp}	R_{ck}^{d}	**Ti**
Humidity spot							
Deteriorated Concrete							
Spalling							
Rusted reinforcements							
Web fracture							
Horizontal cracks							
Vertical cracks							
Inclined cracks							
Rusted stirrups							
Deformed reinforcements							
Construction joint deterioration							
Impact damages							
Support damages – top edge							
Support damages – bottom edge							
Out of plumb							

Table A5. Abutment damage identification form.

Damage	B	K_2	K_3	L	R_{ck}^{exp}	R_{ck}^{d}	Ti
Humidity spot							
Deteriorated Concrete							
Beam/Slab joint deterioration							
Freezing							
De-icing salts							
Spalling							
Reinforcements corrosion							
Tendons corrosion							
Duct deficiency							
Web fracture							
Longitudinal cracks							
Vertical cracks							
Inclined cracks							
Rusted stirrups							
Deformed reinforcements							
Construction joint deterioration							
Impact damages							

Table A6. Beam damage identification form.

Damage	B	K_2	K_3	L	R_{ck}^{exp}	R_{ck}^{d}	Ti
Humidity spot							
Deteriorated Concrete							
Spalling							
Reinforcements corrosion							
Web fracture							
Longitudinal cracks							
Vertical cracks							
Inclined cracks							
Rusted stirrups							
Construction joint deterioration							

Table A7. Slab damage identification form.